AMERICAN MUSEUM NOVITATES

Number 4028, 25 pp. November 6, 2024

A new archaeostomatopod from the Pennsylvanian Wea Shale Member, Nebraska

RUSSELL D.C. BICKNELL,[1] PATRICK M. SMITH,[2] ADIËL A. KLOMPMAKER,[3] AND THOMAS A. HEGNA[4]

ABSTRACT

Mantis shrimp (Stomatopoda) are extant, marine, predatory arthropods, but these malacostracan pancrustaceans are also occasionally preserved in fossil assemblages, particularly in Carboniferous and Cretaceous deposits. Carboniferous species fall into two suborders—Palaeostomatopodea and Archaeostomatopodea—and represent the ancestral forms that gave rise to modern lineages. Herein, we describe hitherto unknown specimens belonging to the archaeostomatopod genus *Tyrannophontes* from the Pennsylvanian-aged Wea Shale Member, eastern Nebraska. We explore the preservation of these fossils using scanning electron microscopy and energy dispersive X-ray spectroscopy. These approaches reveal additional morphological characteristics, including unique appendicular data, such as the earliest occurrence of biramous gilled appendages in Stomatopoda. We suggest that further examination of black shales will likely uncover novel records of these rare pancrustaceans.

[1] Division of Paleontology (Invertebrates), American Museum of Natural History, New York; and Palaeoscience Research Centre, School of Environmental and Rural Science, University of New England, Armidale, Australia.

[2] Department of Biological Sciences, Macquarie University, Sydney, New South Wales; and Palaeontology Department, Australian Museum Research Institute, Sydney, New South Wales.

[3] Department of Museum Research and Collections, University of Alabama, Tuscaloosa, and Alabama Museum of Natural History, University of Alabama, Tuscaloosa.

[4] Department of Geology and Environmental Sciences, State University of New York at Fredonia.

 ISSN 0003-0082

INTRODUCTION

Mantis shrimp (Stomatopoda Latreille, 1817) are a group of marine malacostracans that have a modern diversity of over 520, primarily tropical species (Hof, 1998a; Haug et al., 2010; Schram and Koenemann, 2021; Smith et al., 2023). The group is especially well known for their highly modified and specialized, anterior thoracic appendages—maxillipeds—that are used for predation (Schram, 1979a; Hof, 1998a; Watling et al., 2000; Patek and Caldwell, 2005; Haug et al., 2010; Patek et al., 2013). These unique maxillipeds have two types of attacking morphologies observed in modern forms: spears and clubs (Patek and Caldwell, 2005; Patek et al., 2013; Schram and Koenemann, 2021). Mantis shrimp have also been documented from fossil deposits extending back to the Mississippian (Schram, 2007; Schram and Koenemann, 2021). They have a relatively low preservational potential among arthropods, as has been demonstrated experimentally (Klompmaker et al., 2017), explaining their uncommon occurrence in the fossil record. Based on the present record, stomatopods diversified during the Carboniferous (Smith et al., 2023), have a relatively sparse fossil record between the Carboniferous and the Cretaceous (Schram, 1969b; 1979a; 2007; Haug et al., 2010; Schram, 2010; Haug and Haug, 2021), and experienced a late Mesozoic diversification event (Hof, 1998b; Ahyong et al., 2007; Smith et al., 2023).

Carboniferous mantis shrimp are grouped into Palaeostomatopodea Brooks, 1962, and Archaeostomatopodea Schram, 1969b (Hof, 1998a; Watling et al., 2000; Schram, 2007; Haug et al., 2010; Schram, 2010). Within these two suborders, there are five families, seven genera, and 14 species (Smith et al., 2023). These groups are considered to have exhibited predatory, spearing life modes (Schram, 1969b; 1979a; Brett and Walker, 2002; Haug and Haug, 2021) and gave rise to modern lineages. Carboniferous mantis shrimp have been documented from siderite nodules (Schram, 1969b; 1979a; 2007; Racheboeuf et al., 2009), black shales (Schram, 1979a; 1984), and a plattenkalk limestone (Jenner et al., 1998), reflecting a range of preservational conditions (Schram, 1969b; 1979a; 2007; Schram and Koenemann, 2021). To more thoroughly document and understand Carboniferous stomatopods, we studied novel material from the Pennsylvanian-aged Wea Shale Member, eastern Nebraska. This record presents new insight into the paleoecology of the Wea Shale Member biota and diversity of Carboniferous mantis shrimp.

GEOLOGICAL CONTEXT

The material reported herein comes from the site of the former "Hansen Quarry, Quarry 6" on Route 370 between the towns of Papillion and Bellevue, Sarpy County, Nebraska, within the Wea Shale Member of the Cherryvale Shale (sensu Pope and Marshall, 2010). The Wea Shale Member sits stratigraphically between the Block Limestone Member (underlying), and the Westerville Limestone Member (overlying) (Moore, 1933; Newell, 1935). The unit is primarily a thin sequence of olive-green to gray (or sometimes black) calcareous, clay-rich shales with rare thin argillaceous limestone lenses (Hershey et al., 1960). It ranges from 0.9 m to over 8 m in thickness (Heckel and Watney, 2002), and contains a relatively diverse

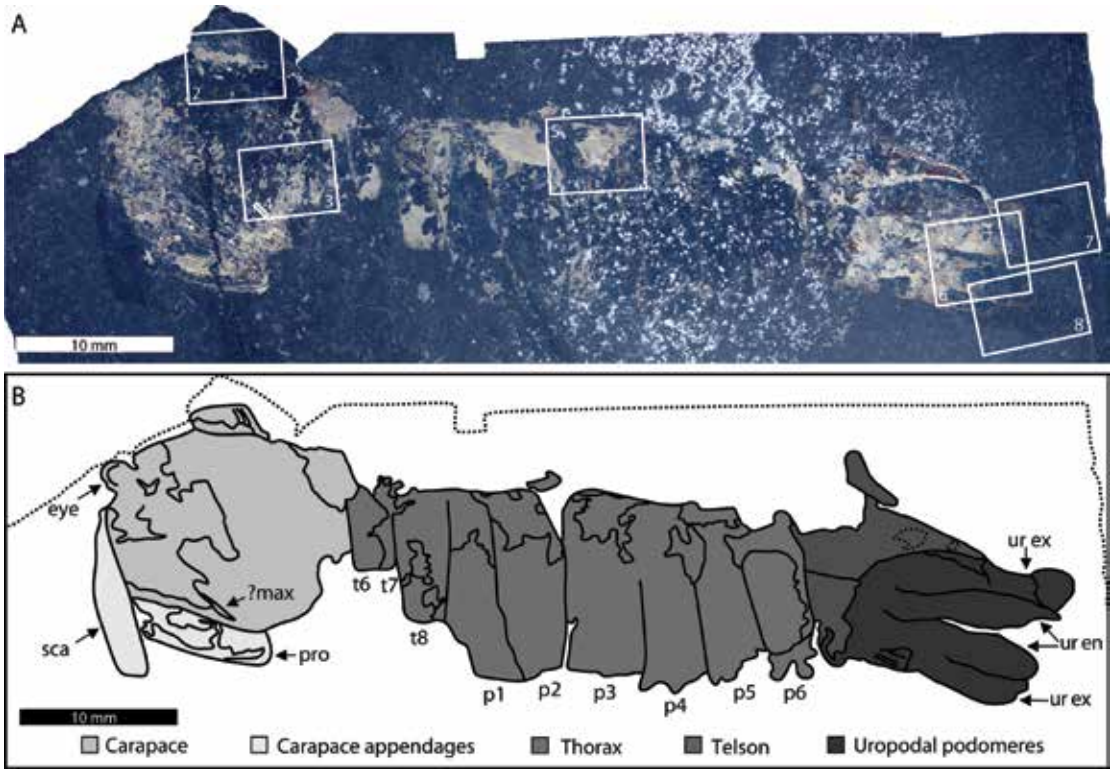

FIGURE 1. Depiction of AMNH-FI-69357. **A.** Complete specimen as preserved. Boxes show areas that are imaged using SEM and EDS maps in figures 2–8. **B.** Line drawing of specimen. Abbreviations: **eye,** compound eye; **max,** maxilliped; **pro,** propodus; **sca,** scaphocerite; **t,** thoracic segment; **p,** pleon segment; **ur en,** uropodal endopod; **ur ex,** uropodal exopod. Numbers 1–8 indicate thoracic and pleon segment numbers; ? indicates uncertain assignment of the structure. Image credit: Thomas Hegna.

fauna, including jellyfish, brachiopods, bivalves, gastropods, bryozoans, crinoids, algae, as well as numerous shark and fish species (Ossian, 1973; Zangerl and Case, 1973; Williams, 1985; Monson, 2010). While some of the shelly fauna are partially silicified, most fossils are preserved as delicate carbon films (Monson, 2010).

The basal fossiliferous portion of the Wea Shale Member represents the maximum flooding surface for the entire Cherryvale Shale. However, unlike the offshore black shales of the major cyclothems in the American Midcontinent and Illinois basins, the unit lacks a black phosphatic facies at its base. This, along with the fauna (Heckel and Baesemann, 1975), suggests a relatively shallow, offshore marine depositional environment (Heckel, 1992). The abundant idiognathodid-dominated conodont fauna (Gunnell, 1933) places the Wea Shale Member in the Cherryvale cyclothem and the *Streptognathodus gracilis* conodont Zone. This zone is within the early to middle Missourian Stage (Barrick et al., 2022, and references therein) and is approximately equivalent to the Late Pennsylvanian Kasimovian Stage (approximately 303.7–307 mya) on the global scale (Lucas et al., 2022a; 2022b).

METHODS

The two examined specimens are housed within the American Museum of Natural History, New York (prefix AMNH-FI) invertebrate paleontology collection. They have been assigned specimen numbers AMNH-FI-69356, 69357. The specimens were imaged with a Cannon EOS Mark II 6D with a MP-E 65 mm lens set up as part of a Macropod stackshot system under LED lights. Close up images were composed of multiple images taken at different depths of field and digitally stacked using Zerene Stacker to create one, hyperfocused image. Specimens were measured with a pair of digital calipers. Isolated conodont elements were observed on the shale surfaces.

To examine the elemental composition and possible preservational mode of AMNH-FI-69356 and 69357, the specimens were examined using Scanning Electron Microscopy (SEM) and Energy Dispersive X-Ray Spectroscopy (EDS). Specimens were analyzed, uncoated, under low vacuum (30 kPa), nitrogen conditions at a voltage of 20 kV and an amperage of 3 nA, using a Tescan Vega S5124 at SUNY Fredonia to collect back scatter electron (BSE) images. Elemental map images were gathered using an Oxford Ultimax 65 mm detector at a resolution of 4096K pixels, processed and exported on AZtec software (version 6.1/Oxford).

When describing these specimens, we followed the morphology terminology of Schram (1969b; 1979a; 2007) and the systematic paleontology of Schram (1969b; 1979a; 2007) and Smith et al. (2023).

SYSTEMATIC PALEONTOLOGY

Order Stomatopoda Latreille, 1817

Suborder Archaeostomatopodea Schram, 1969b

Family Tyrannophontidae Schram, 1969b

Genus ?*Tyrannophontes* Schram, 1969b

Type species *Tyrannophontes theridion* Schram, 1969b

Figures 1–17

Examined material: AMNH-FI-69357; AMNH-FI-69356.

Description: AMNH-FI-69357 (figs. 1–8): Incomplete eumalacostracan preserved in lateral view. All body sections preserved as flattened impression in black shale. Carapace, scaphocerite, raptorial appendages, and eyes are present. Three thoracic segments and six pleonal segments observed. Uropodal endopod and exopod present. Telson, triangular, spikelike morphology.

Carapace: Carapace is laterally compressed, appearing subrounded in lateral view. Compound eyes are subrounded.

Scaphocerite: Platelike morphology, 10.8 mm long, 0.4 mm wide dorsally, increasing to 2 mm wide ventrally (fig. 1). No spines noted. Preserved as impression, no evidence of cuticle.

TABLE 1. Measurements of thoracic and pleonal segments. Measurements in mm. – indicates that this structure could not be measured in the fossil.

	Thoracic segment 6	Thoracic segment 7	Thoracic segment 8	Pleonal segment 1	Pleonal segment 2	Pleonal segment 3	Pleonal segment 4	Pleonal segment 5	Pleonal segment 6
				AMNH-FI-69357					
Length	5.2	5.8	8.3	12.0	12.2	12.0	12.3	11.1	10.7
Width	2.6	1.4	3.5	3.8	4.5	4.8	3.5	3.6	3.9
				AMNH-FI-69356					
Length	–	–	–	–	–	–	8.1	8.4	6.6
Width	–	–	–	–	–	–	1.4	3.6	2.7

Raptorial appendages: Propodus of hypertrophied maxilliped II appendage observed (fig. 1). No spines present. Toothlike structures observed as impressions through carapace under SEM (fig. 4). These may represent spines of maxillipeds III–V.

Thorax: Segments posterior to carapace are interpreted as thoracic segments 6–8. Fifth segment is possibly obscured by carapace. Segments are rectangular and anterior segments are narrower, with anteriormost segment reduced in width by 38.4% compared to pleonal segment 1 (table 1). Length is also reduced by ~30%–50% compared to pleonal segments, reflecting incomplete preservation (figs. 1, 5). Cuticular regions observed as cream or dark yellow portions.

Pleon: Six segments anterior to telson are considered first to sixth pleonal segments. All segments are rectangular, four times longer than wide (table 1). No anatomical information other than segment boundaries and cuticle are observed.

Pleonal appendages: Uropodal endopods and exopods approximately same size, prominent, elongated, paddle shaped, with rounded edges (figs. 1, 6–8). No evidence for setae or spines, but distal regions less cuticularized than proximal regions. Basipod, endopod, and exopod insertions not determined.

Telson: Telson partly preserved (fig. 1). Anteriorly broad and triangular, tapering posteriorly. No ridges or keel.

Description: AMNH-FI-69356 (figs. 9–17): Incomplete eumalacostracan preserved in lateral view in black shale. Carapace, raptorial appendages, and eyes present. No thoracic segments are confidently determined, three posterior pleonal segments noted. Pleopod gills preserved. Possible telson fragment observed.

Carapace: Carapace is laterally compressed, appears subrounded in lateral view (figs. 9, 10, 13, 15). Compound eyes are subround (fig. 10).

Raptorial appendages: Propodus of maxilliped II appendage observed (figs. 9, 12, 14, 16). No spines noted. Possible maxilliped II merus noted. Cuticle fragments associated with fossil interpreted as possible remains of maxillipeds III and IV.

Pleon: Three segments anterior to telson are considered to represent the fourth to sixth pleonal segments (fig. 9). Segments are fragmented, but subrectangular in morphology, approx-

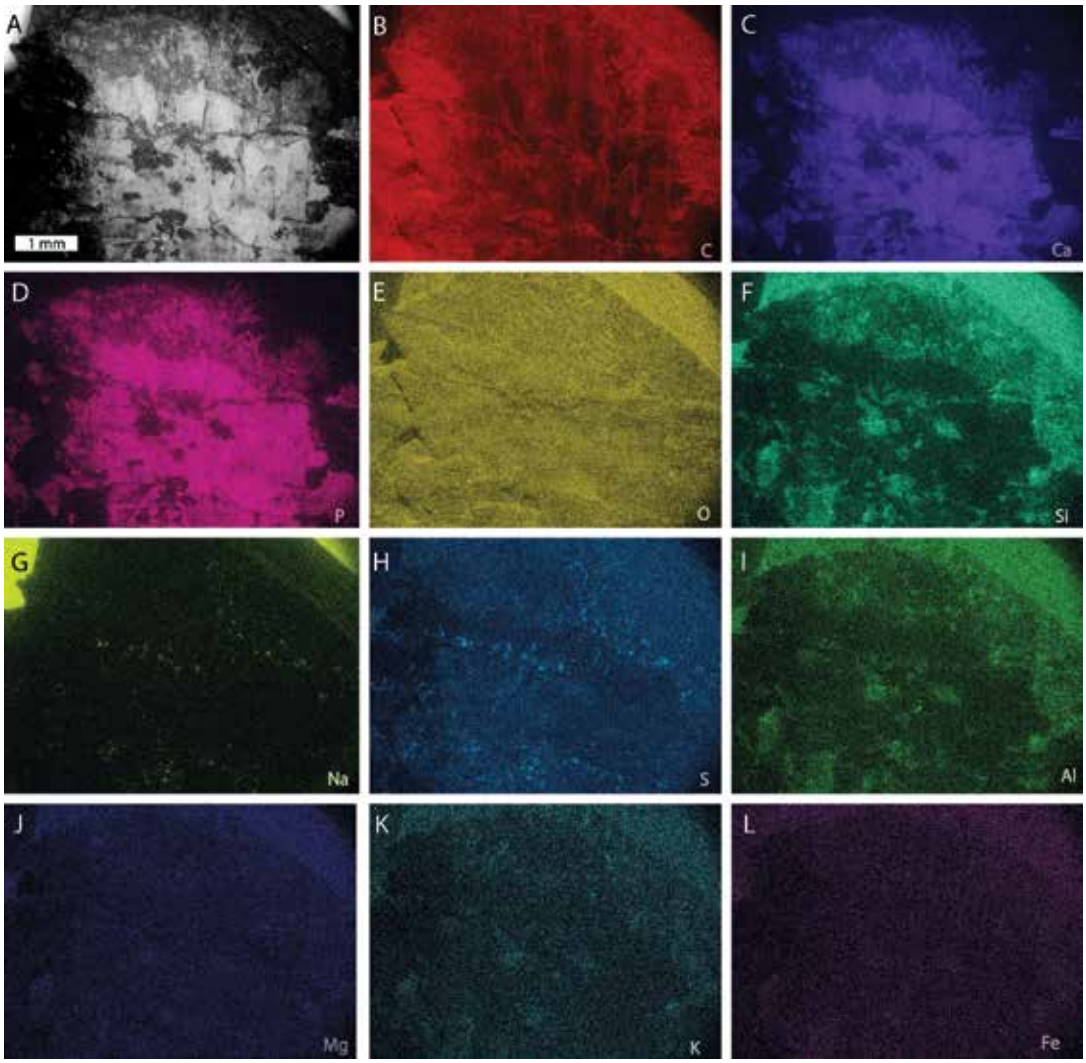

FIGURE 2. SEM backscatter image and EDS elemental maps of dorsal carapace; area indicated in figure 1A. **A.** Backscatter image of dorsal carapace. **B–L.** Elemental maps of carbon, calcium, phosphorus, oxygen, silica, sodium, sulphur, aluminum, magnesium, potassium, and iron, respectively.

imately four times longer than wide (table 1). No additional anatomical information can be determined.

Pleonal appendages: Pleopod gills observed, large, bladelike (figs. 9, 17). Based on position, they could be associated with first or second pleonal segment.

Telson: Telson partly preserved and fragmentary.

Remarks: Pennsylvanian archaeostomatopods consist of four genera: *Daidal* Schram, 2007, *Gorgonophontes* Schram, 1984, *Chabardella* Racheboeuf et al., 2009, and *Tyrannophontes* Schram, 1969b (Schram, 2007; Smith et al., 2023). We use these four to explore our placement of the Wea Shale Member material in *Tyrannophontes*.

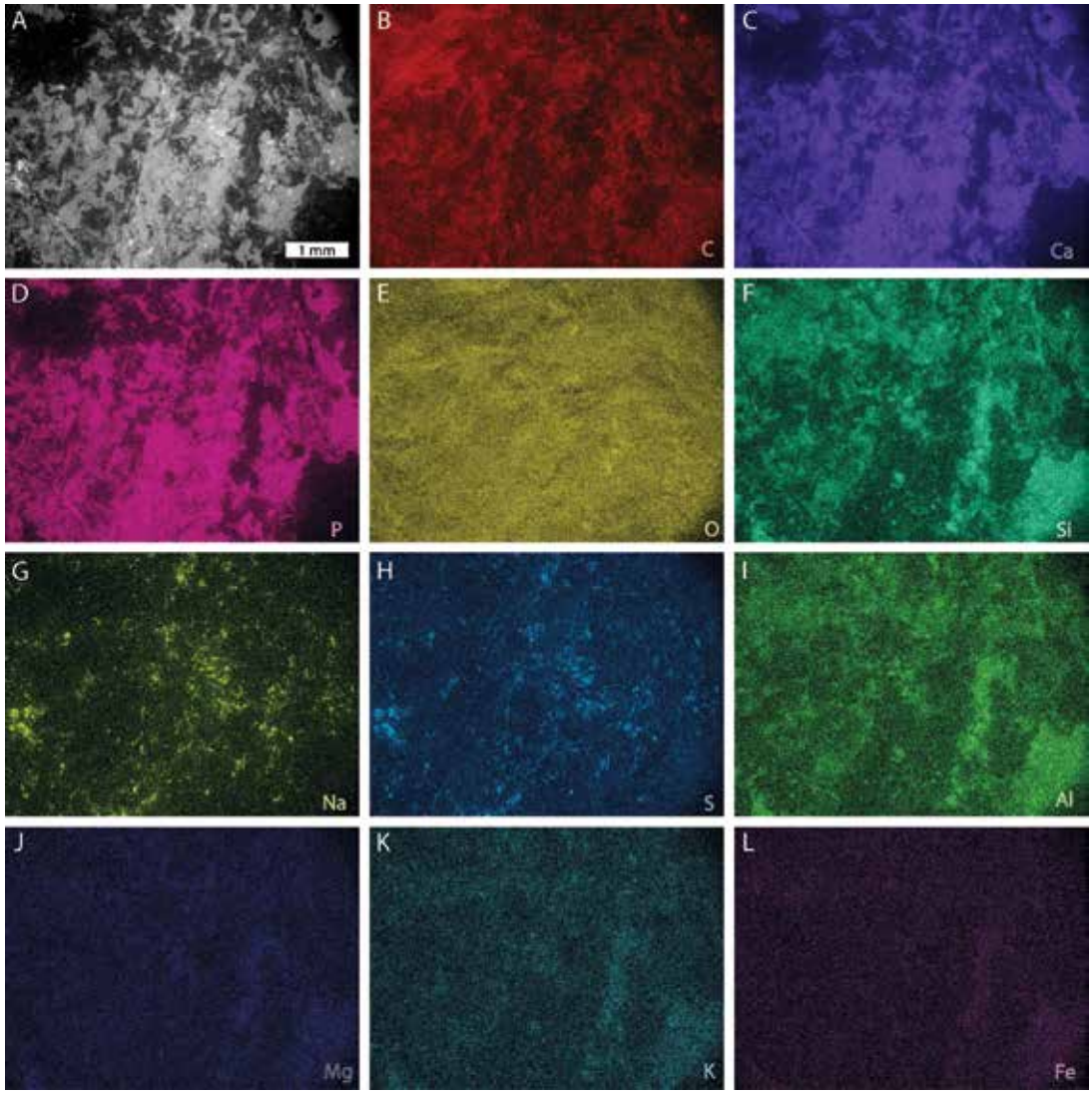

FIGURE 3. SEM backscatter image and EDS elemental maps of posterior carapace; area indicated in figure 1A. **A.** Backscatter image of exoskeleton. **B–L.** Elemental maps of carbon, calcium, phosphorus, oxygen, silica, sodium, sulphur, aluminum, magnesium, potassium, and iron, respectively.

Daidal is an archaeostomatopod with maxillipeds II–V of similar size, with spines along the uropodal regions, and commonly with uropodal exopods and endopods with setae (Schram, 2007; Smith et al., 2023). Our specimens show no evidence for uropodal setae and AMNH-FI-69356 suggests that maxilliped II was larger than III–V. We therefore do not assign our material to *Daidal*.

Gorgonophontes has alternating robust and reduced spines on the propodi; a broad triangular telson with a sharp point, and distally located movable telson spines; and uropodal exopods and endopods with setae (Schram, 2007; Haug and Haug, 2021; Smith et al., 2023). None

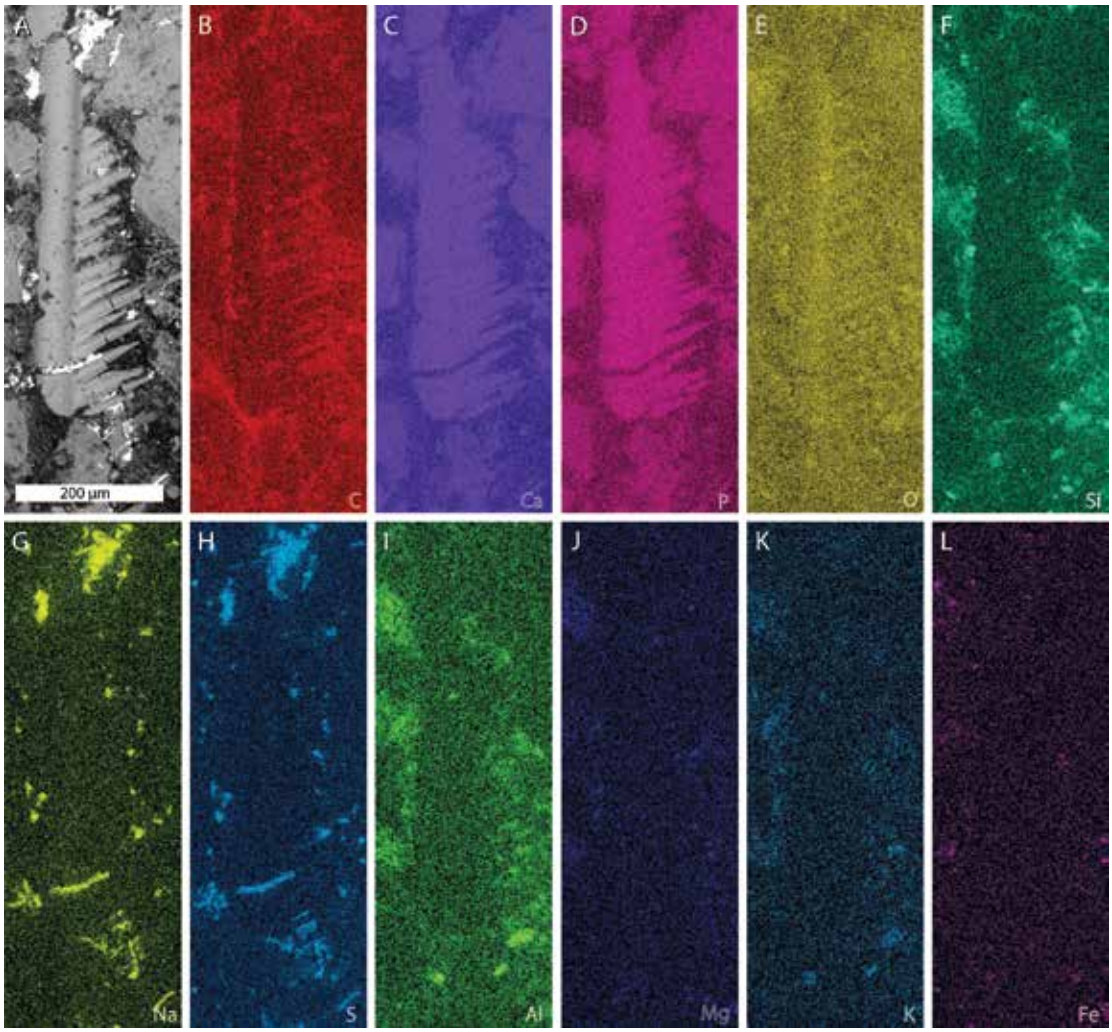

FIGURE 4. SEM backscatter image and EDS elemental maps of possible propodus; area indicated in figure 1A. **A.** Backscatter image of propodus. **B–L.** Elemental maps of carbon, calcium, phosphorus, oxygen, silica, sodium, sulphur, aluminum, magnesium, potassium, and iron, respectively.

of these morphologies are observed in our material. In particular, proposed propodal spines are of consistent length (fig. 4), and the uropodal exopods and endopods lack setae. We therefore cannot ascribe the Wea Shale Member specimens to *Gorgonophontes*.

Chabardella has spines along the posterior margins of thoracic and pleonal segments, and a reduced telson (Schram, 2007). These morphologies are not observed in our material, excluding the Wea Shale Member fossils from *Chabardella*.

Tyrannophontes has a carpus forming a ballistic joint, a larger maxilliped II, uropodal endopods and exopods lacking setae, and a subtriangular telson with moveable spines (Schram, 2007). Our material does not fully conform to this description—we do not have evidence for a carpus or moveable spines on the telson. These are either not preserved or may be laterally

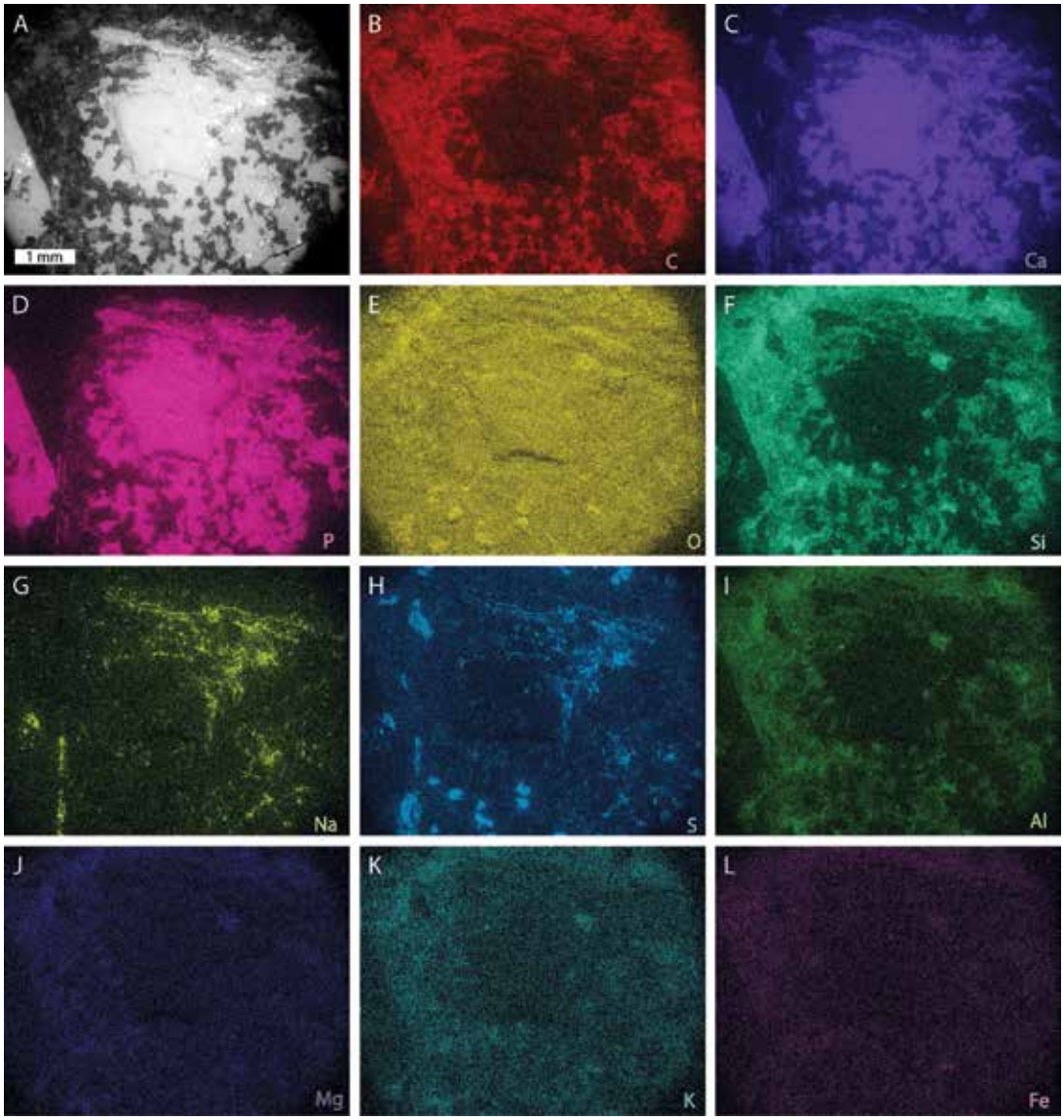

FIGURE 5. SEM backscatter image and EDS elemental maps of dorsal pleonal segment 3; area indicated in figure 1A. **A.** Backscatter image of segment. **B–L.** Elemental maps of carbon, calcium, phosphorus, oxygen, silica, sodium, sulphur, aluminum, magnesium, potassium, and iron, respectively.

compressed. However, our material exhibits a large maxilliped II, uropodal endopods and exopods without setae, and a subtriangular telson in lateral view. As such, we tentatively place this material into *Tyrannophontes*, but refrain from a species designation at present due to insufficient preservation.

Genera within Palaeostomatopodea must also be considered, as these forms are known from Carboniferous deposits (Smith et al., 2023). The three palaeostomatopod genera are *Archaeocaris* Meek, 1871, *Bairdops* Schram, 1979a, and *Perimecturus* Peach, 1881

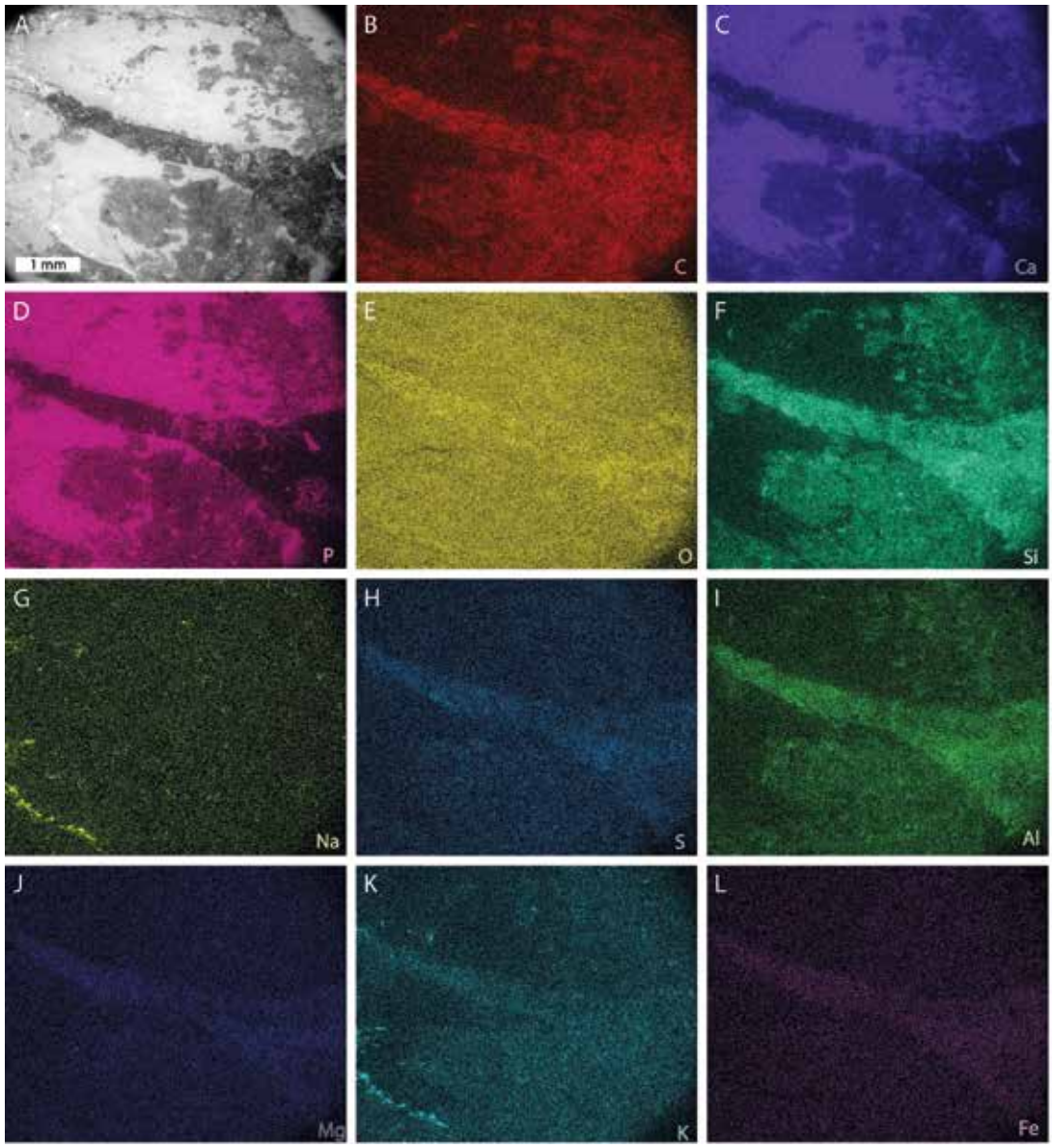

FIGURE 6. SEM backscatter image and EDS elemental maps of proximal uropodal endopod; area indicated in figure 1A. **A.** Backscatter image of endopod. **B–L.** Elemental maps of carbon, calcium, phosphorus, oxygen, silica, sodium, sulphur, aluminum, magnesium, potassium, and iron, respectively.

Among other synapomorphies, *Archaeocaris* is defined as having an ovoid telson (Schram, 1979a; 2008). In the examined material, the telson is broad and triangular. We therefore exclude our material from *Archaeocaris*.

Bairdops has a rectangular carapace that extends posteriorly to the eighth thoracic segment, bladelike uropodal podomeres, and reduced raptorial appendages (Schram, 1979a; Briggs and

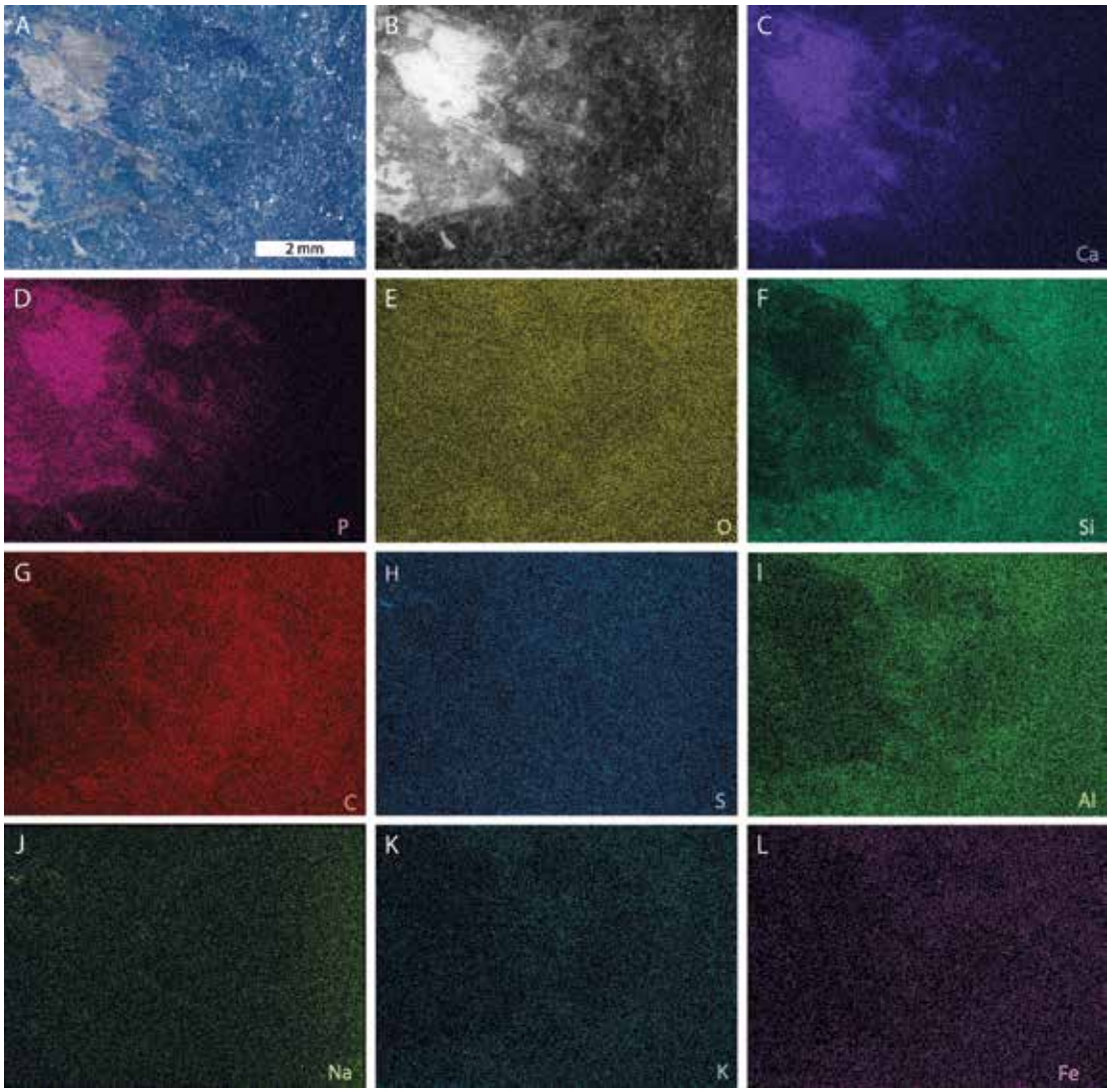

FIGURE 7. Light and SEM backscatter imagery and EDS elemental maps of distal uropodal exopod; area indicated in figure 1A. **A.** Exopod under LED lighting. **B.** Backscatter image of exopod. **C–L.** Elemental maps of calcium, phosphorus, oxygen, silica, carbon, sulphur, aluminum, sodium, potassium, and iron, respectively.

Clarkson, 1985; Jenner et al., 1998). These morphologies are not observed in the Wea Shale Member material, excluding it from *Bairdops*.

Perimecturus has a broad, triangular telson, bladelike uropodal exopods, and reduced uropodal endopods. The telson morphology is similar in the Wea Shale material. However, the uropodal morphologies are markedly different. As such, we exclude the Wea Shale Member specimens from *Perimecturus*.

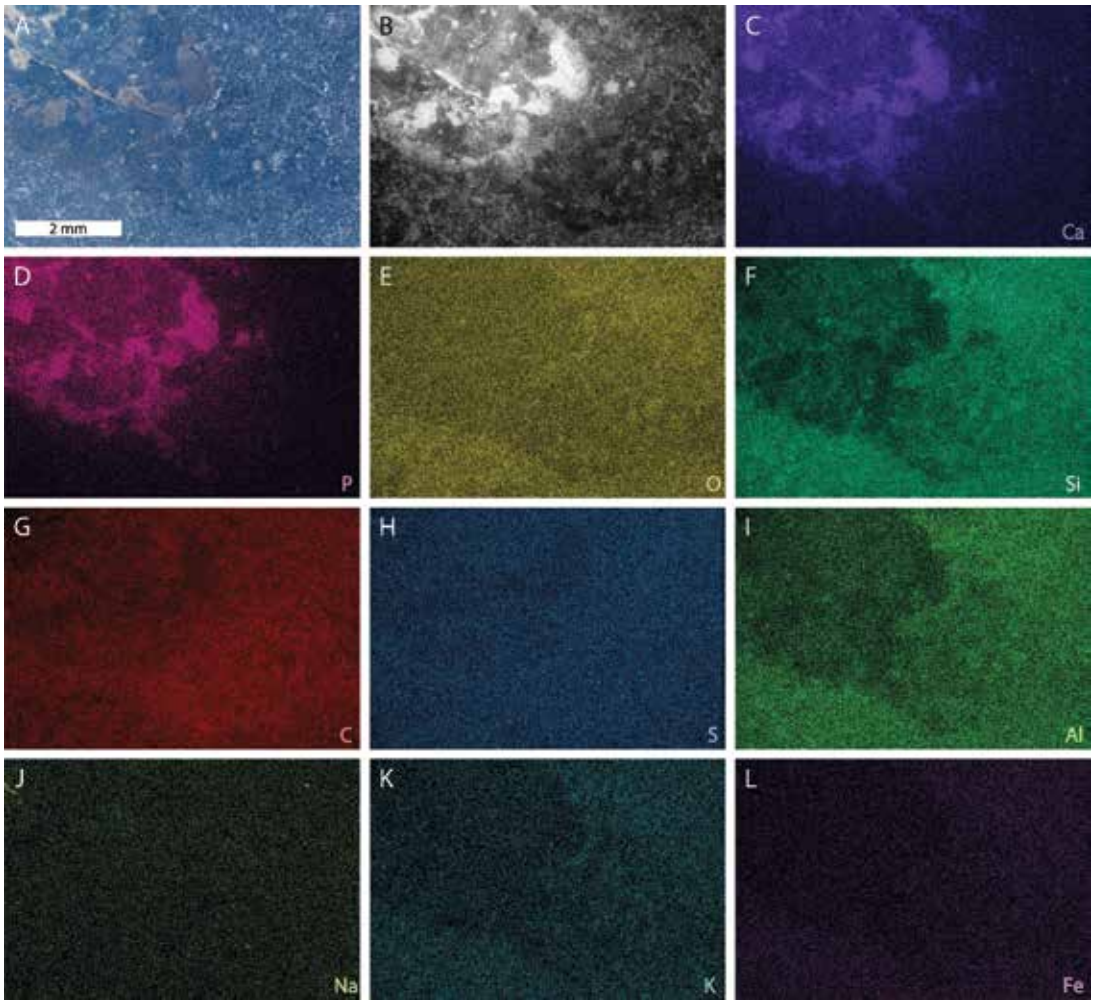

FIGURE 8. Light and SEM backscatter imagery and EDS elemental maps of distal region uropodal endo- and exopods; area indicated in figure1A. **A.** Appendages under LED lighting. **B.** Backscatter image of appendage sections. **C–L.** Elemental maps of calcium, phosphorus, oxygen, silica, carbon, sulphur, aluminum, sodium, potassium, and iron, respectively.

RESULTS

The elemental maps of both specimens highlight preservational aspects of the exoskeleton, lateral compound eyes, appendages, and the matrix (figs. 2–8, 10–17). The exoskeletal sections show enrichment in calcium and phosphorus (figs. 2C, D; 3C, D; 5C, D; 6C, D; 7C, D; 8C, D; 11C, D; 15C, D) with limited enrichment in carbon and silica (figs. 2B, F; 3B, F; 5B, F; 6B, F; 7F, G; 8F, G; 11B, F; 15B, F). The maxilliped podomeres show similar enrichment in calcium and phosphorus (figs. 4C, D; 12C, D; 14C, D 16C, D). The compound eyes show enrichment in calcium and phosphorus (fig. 10C, D) and the eye margins

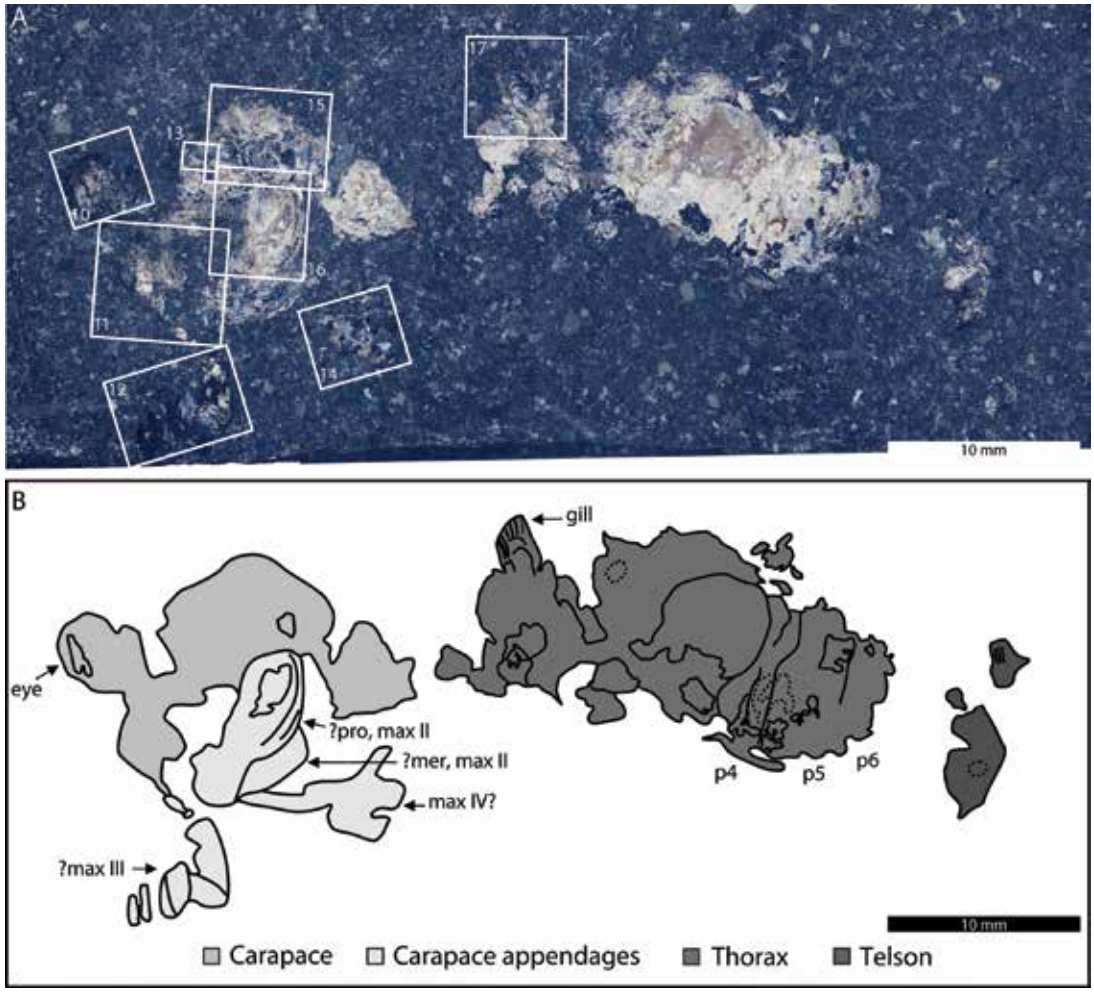

FIGURE 9. Depiction of AMNH-FI-69356. **A.** Complete specimen as preserved. Boxes show areas that are imaged using SEM and EDS maps in figures 10–17. **B.** Line drawing of specimen. Abbreviations: **eye,** compound eye; **gill,** pleon gill; **max,** maxilliped; **mer,** merus; **p,** pleon segment; **pro,** propodus. Numbers (4–6) indicate pleon segment numbers. Roman numerals (II–IV) indicate raptorial appendage numbers. ? indicates uncertain assignment of the structure. Image credit: Thomas Hegna.

show limited carbon enrichment (fig. 10B). The uropodal endopods and exopods show enrichment in calcium and phosphorus (figs. 6C, D; 7C, D; 8C, D) and enrichment in silica along the distal regions (fig. 8F). The pleonal gills show marked enrichment in calcium and phosphorus (fig. 17C, D). Magnesium and iron are occasionally prevalent, mostly proximal to appendage margins (figs. 6J, L; 17L). Small regions of enriched sulfur and sodium are noted variably within exoskeletal regions (figs. 3G, H; 5G, H; 10G, H; 11G, H; 13G, H; 16H, I). There is pervasive enrichment of oxygen, silica, aluminum, and potassium in the matrix around the fossils (figs. 2–8, 10–17).

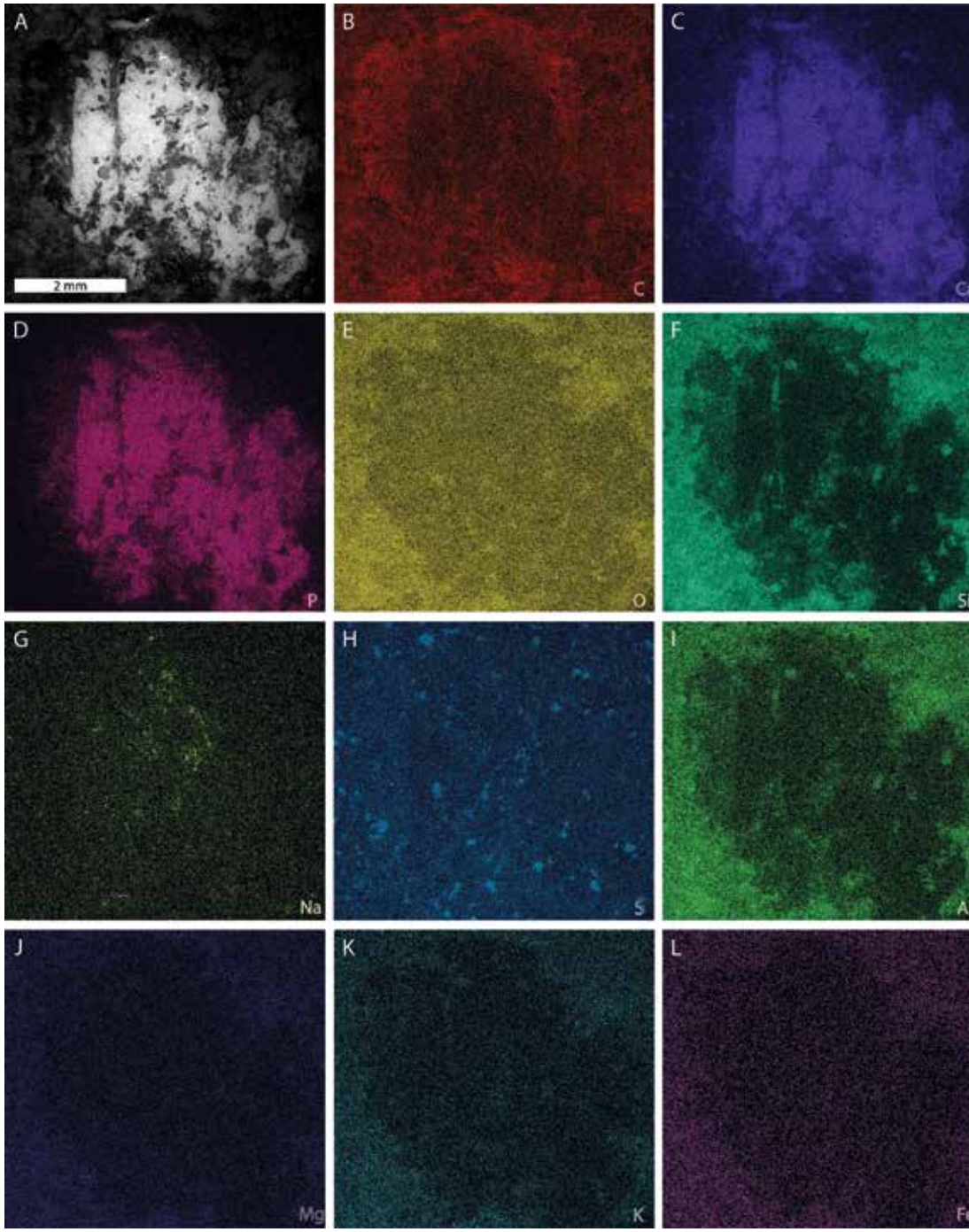

FIGURE 10. SEM backscatter image and EDS elemental maps of compound eye region; area indicated in figure 9A. **A.** Backscatter image of eye. **B–L.** Elemental maps of carbon, calcium, phosphorus, oxygen, silica, sodium, sulphur, aluminum, magnesium, potassium, and iron, respectively.

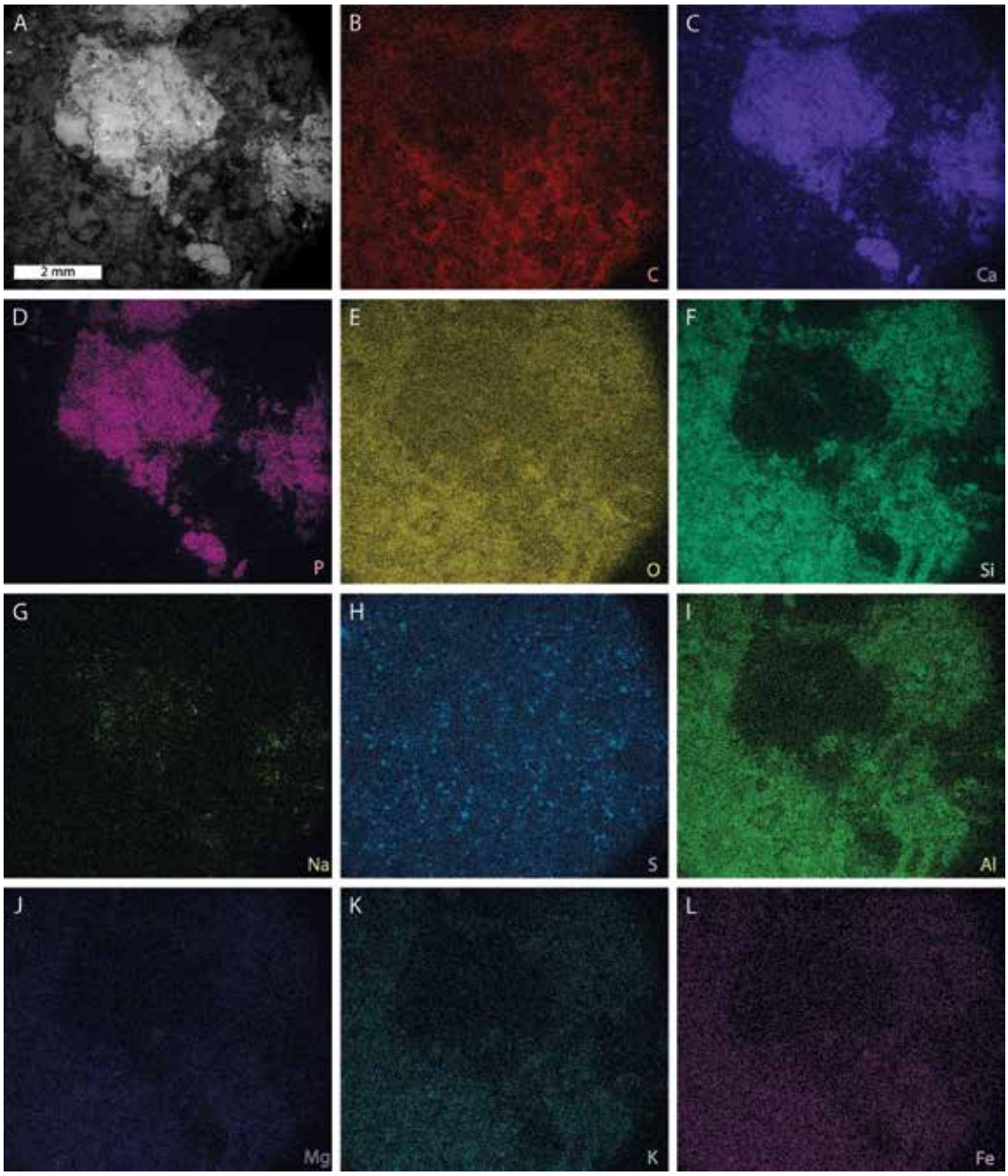

FIGURE 11. SEM backscatter image and EDS elemental maps of anterior carapace; area indicated in figure 9A. **A.** Backscatter image of carapace. **B–L.** Elemental maps of carbon, calcium, phosphorus, oxygen, silica, sodium, sulphur, aluminum, magnesium, potassium, and iron, respectively.

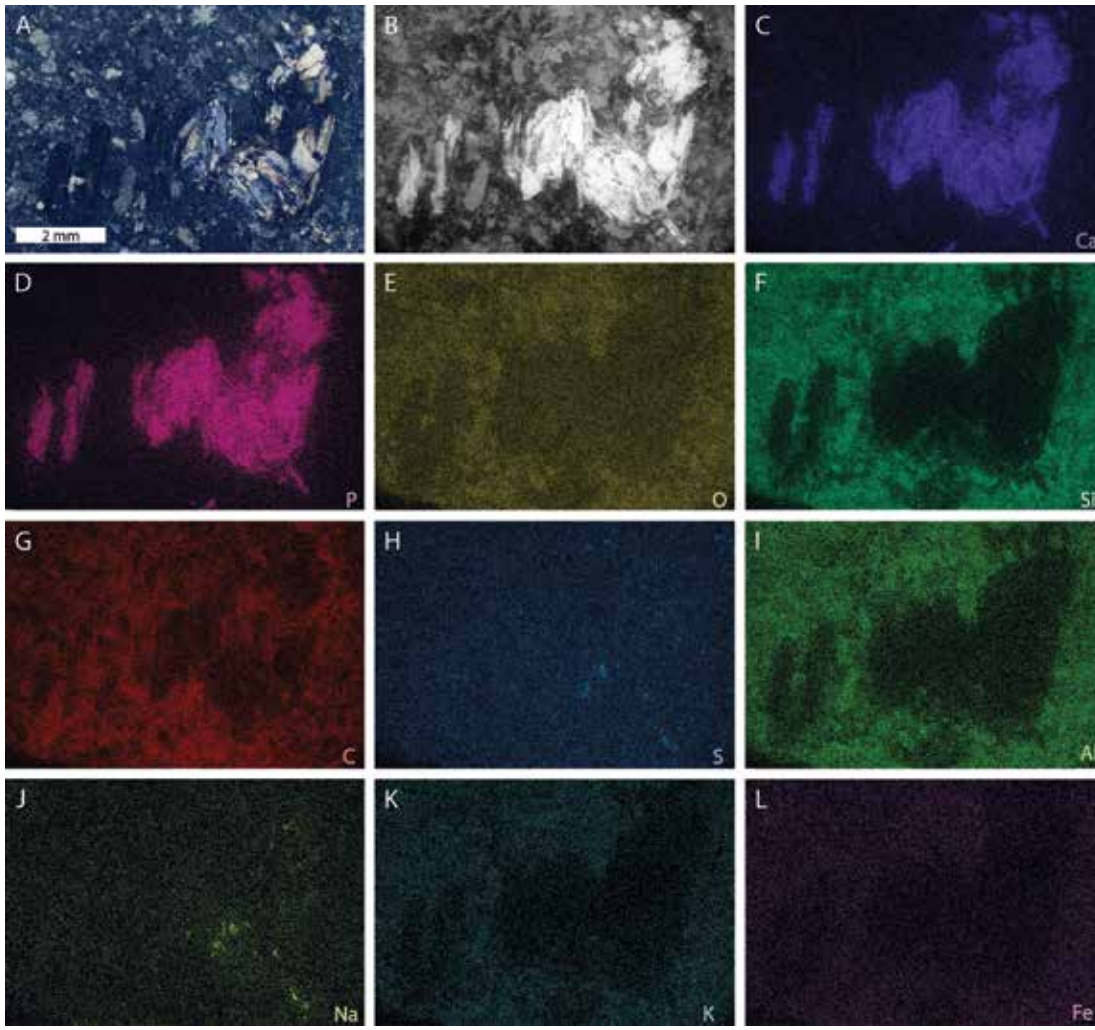

FIGURE 12. Light and SEM backscatter imagery and EDS elemental maps of possible maxilliped III; area indicated in figure 9A. **A.** Appendages under LED lighting. **B.** Backscatter image of appendage region. **C–L.** Elemental maps of calcium, phosphorus, oxygen, silica, carbon, sulphur, aluminum, sodium, potassium, and iron, respectively.

DISCUSSION

Taphonomy and Preservation

The elemental composition of fossil mantis shrimp has not been explored in extensive detail. As such, comparisons with other arthropods are needed. Enrichment in calcium and phosphorus in cuticular regions likely represent original calcium phosphate, common for pan-crustacean material (Martill, 1988; Briggs and Wilby, 1996; Wilby and Briggs, 1997; Jauvion et al, 2020). The slightly elevated presence of magnesium and iron along appendage margins may reflect adherence to, or possible complete replacement of, soft tissues with illite-group clay

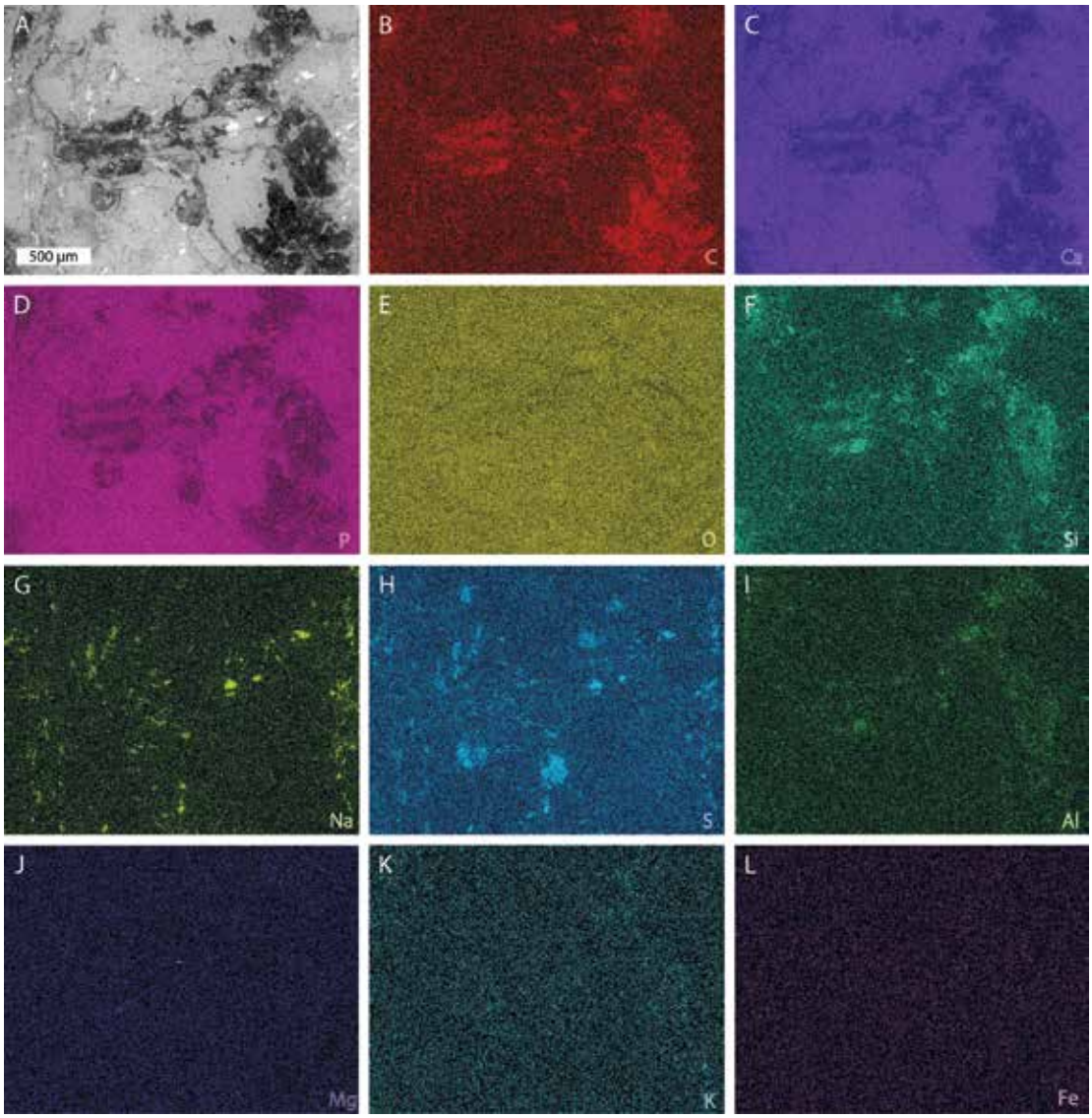

FIGURE 13. SEM backscatter image and EDS elemental maps of carbon and silica rich region in carapace; area indicated in figure 9A. **A.** Backscatter image of region. **B–L.** Elemental maps of carbon, calcium, phosphorus, oxygen, silica, sodium, sulphur, aluminum, magnesium, potassium, and iron, respectively.

minerals, comparable to preservation in the "middle" Cambrian Burgess Shale (Orr et al., 1998), or Upper Ordovician Soom Shale (Gabbott et al., 2001). The oxygen, silica, aluminum, and potassium within the rock matrix is typical of black shale elemental construction (Wortmann et al., 1999). These conditions result in fossils that appear preservationally similar to *Gorgonophontes peleron* Schram, 1984 (Schram, 2007), suggesting mantis shrimp, and likely other arthropods, preserved in black shales follow similar taphonomic pathways.

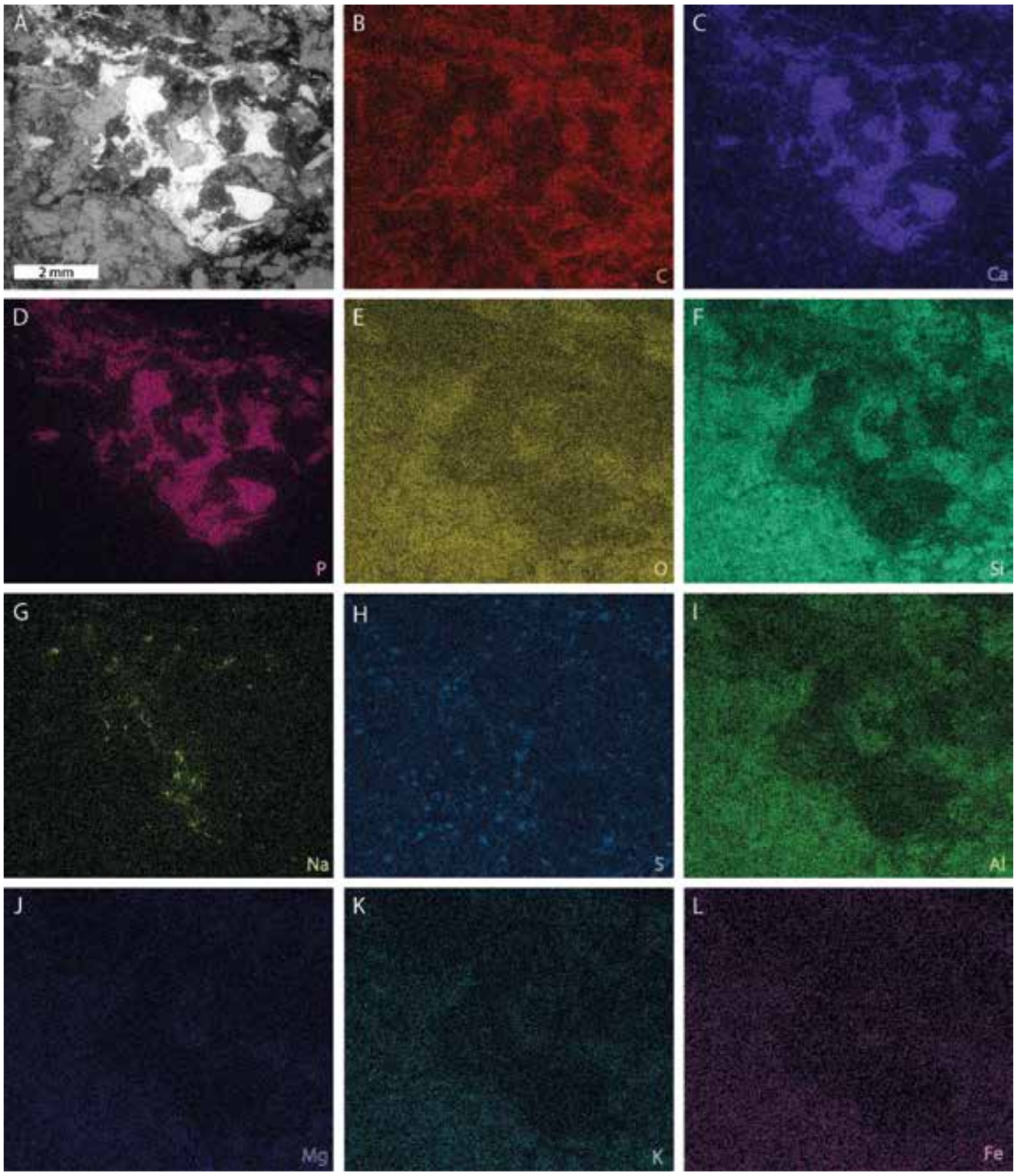

FIGURE 14. SEM backscatter image and EDS elemental maps of possible maxilliped IV; area indicated in figure 9A. **A.** Backscatter image of appendage. **B–L.** Elemental maps of carbon, calcium, phosphorus, oxygen, silica, sodium, sulphur, aluminum, magnesium, potassium, and iron, respectively.

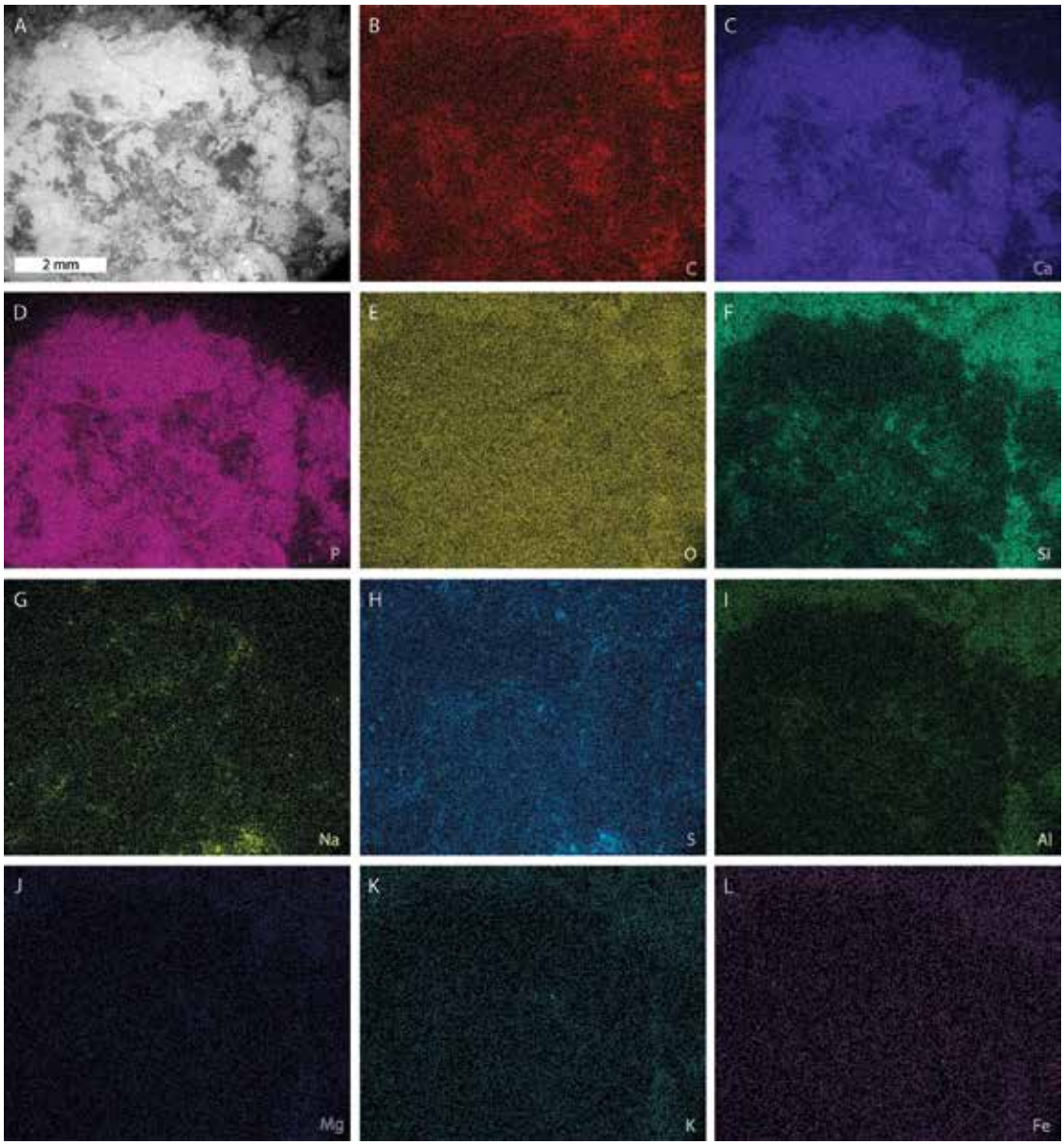

FIGURE 15. SEM backscatter image and EDS elemental maps of dorsal carapace; area indicated in figure 9A. **A.** Backscatter image of carapace. **B–L.** Elemental maps of carbon, calcium, phosphorus, oxygen, silica, sodium, sulphur, aluminum, magnesium, potassium, and iron, respectively.

The co-occurrence of sodium and sulfur enrichment remains unexplained. As Na_2S and Na_2SO_4 both have uses in modern textile, chemical, and energy industries (Nimchik et al., 2024), we are uncertain if these elements represent a diagenetic pathway or contamination.

Stomatopod decay experiments present insight into the degree of decay for AMNH-FI-69356 and 69357 (Hof and Briggs, 1997; Klompmaker et al., 2017). Following Hof and Briggs (1997: fig. 5), we have two stages of decay. AMNH-FI-69357 falls within the "partly complete" category, as the specimen

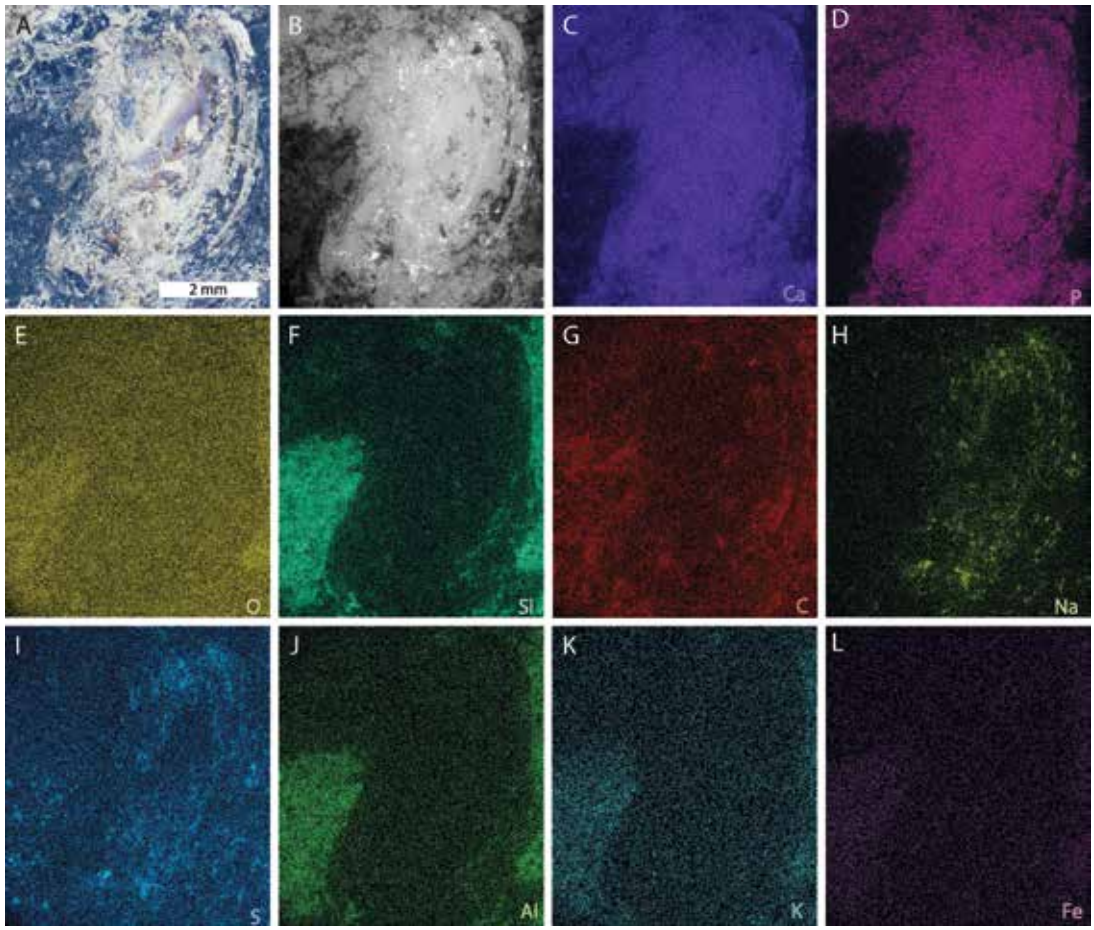

FIGURE 16. Light and SEM backscatter imagery and EDS elemental maps of propodus; area indicated in figure 9A. **A.** Propodus under LED lighting. **B.** Backscatter image of propodus. **C–L.** Elemental maps of calcium, phosphorus, oxygen, silica, carbon, sulphur, aluminum, sodium, potassium, and iron, respectively.

shows limited disarticulation along the thorax and pleon, but the appendage is still articulated to the carapace. Conversely, AMNH-FI-69356 falls into the "fragmentary" condition, showing marked disarticulation of the appendages from the carapace. Given these constraints, the Wea Shale Member mantis shrimp probably experienced decay within an anoxic environment for weeks to months. Interestingly, despite this late stage of decay, unique anatomical data, such as gilled appendages are still preserved, hinting that later stage decay may still record soft, ventrally located morphologies.

Anatomy, Evolution, and Paleoecology

The novel record of an archaeostomatopod within Pennsylvanian black shales highlights an increased fossil record of the group and evidences a more detailed evolutionary history for Carboniferous archaeostomatopods (Smith et al., 2023). Indeed, the Wea Shale Member mate-

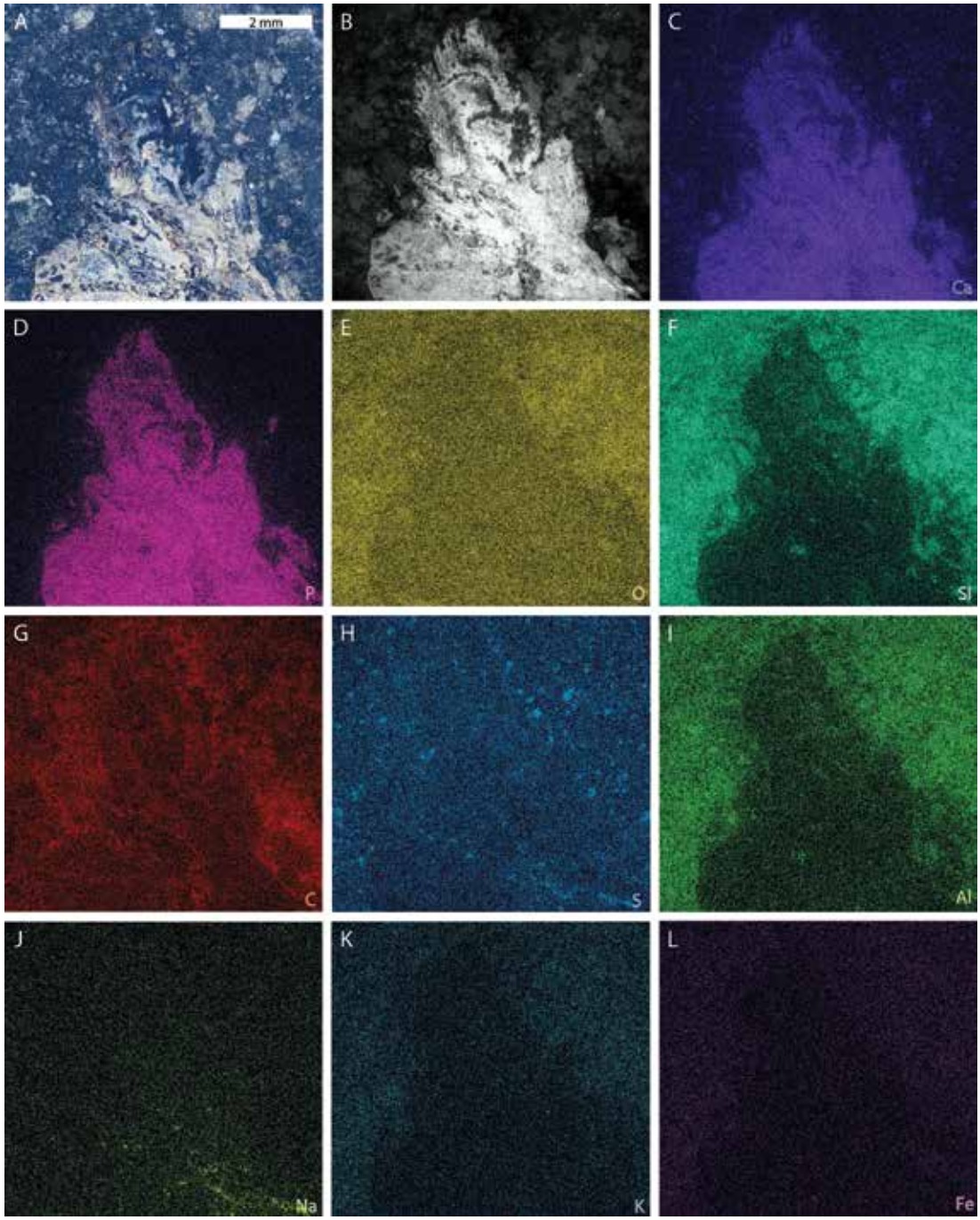

FIGURE 17. Light and SEM backscatter imagery and EDS elemental maps of pleon gill; area indicated in figure 9A. **A.** Gill under LED lighting. **B.** Backscatter image of gill. **C–L.** Elemental maps of calcium, phosphorus, oxygen, silica, carbon, sulphur, aluminum, sodium, potassium, and iron, respectively.

rial here has a distinct morphology, including a large scaphocerite and uropodal sections without setae, indicating it may warrant a new species designation. However, the partial preservation precludes a completely confident generic assessment. Additional collecting of material showing more anatomical information is needed to better understand the taxonomic position within Archaeostomatopodea.

To date, no pleonal gills have been recorded in archaeostomatopods. This unique appendage data demonstrates an exceptional occurrence of biramous gilled appendages in early Stomatopoda. Gilled appendages are used in respiration (Hickman, 1973), a condition that had a Carboniferous or earlier origin. Importantly, these appendages were identified with backscatter electron microscopy, as they were not particularly evident under LED lighting. Future examination of other arthropods preserved similarly may benefit from this additional imaging approach.

Given the structure of the raptorial appendages (particularly the toothlike elements on maxillipeds III–V), it is likely the Wea Shale Member stomatopod was ecologically similar to modern "spearer" species. These stomatopods are ambush predators targeting soft-bodied prey (Schram, 1969a; 1969b; 1979a; 1979b; Caldwell and Childress, 1990). However, known possible prey items (juvenile iniopterygiform fish; Zangerl and Case, 1973; Williams, 1985, and jellyfish *Prothysanostoma eleano* Ossian, 1973) are too large to have been targeted. Annelid worms or naked mollusks may have also been fed upon, but there is currently no evidence they co-occurred. The absence of abundant suitable prey potentially indicates that more soft-bodied organisms (particularly in lower tropic guilds) are yet to be described from the Wea Shale Member.

CONCLUSIONS

We documented novel specimens of archaeostomatopods within the Pennsylvanian-aged Wea Shale Member of Nebraska. While this material is morphologically comparable to *Tyrannophontes*, the fragmentary nature of the fossils precluded a confident specific designation. As such, we placed the material in open nomenclature. Exploring the elemental composition of these specimens highlighted a standard taphonomic pathway for arthropods preserved in black shale, but possible evidence for replacement of soft tissues with illite-group minerals. Furthermore, EDS maps highlighted anatomical details, such as appendage data, that may be overlooked using normal light microscopy, evidencing the impact of EDS mapping in thoroughly documenting fossil arthropods preserved in black shale.

ACKNOWLEDGMENTS

This research was funded by an MAT Program Postdoctoral Fellowship (to R.D.C.B). We thank Bushra Hussaini (AMNH) and Hilary Ketchum (AMNH) for helping with collections. We thank Carl Mehling for suggestions on locality data for the examined specimens. NSF grant EAR 2216215 supported the SEM-EDS system at SUNY Fredonia. Finally, we thank Christopher Smith and Sylvain Charbonnier for constructive reviews that improved the quality of the manuscript.

REFERENCES

Ahyong, S.T., A. Garassino, and B. Gironi. 2007. *Archaeosculda phoenicia* n. gen., n. sp. (Crustacea, Stomatopoda, Pseudosculdidae) from the Upper Cretaceous (Cenomanian) of Lebanon. Atti della Società Italiana di Scienze Naturali e del Museo Civico di Storia Naturale in Milano 148: 3–15.

Barrick, J.E., et al. 2022. Carboniferous conodont biostratigraphy. Geological Society, London, special publication 512: 695–768.

Brett, C.E., and S.E. Walker. 2002. Predators and predation in Paleozoic marine environments. Paleontological Society Papers 8: 93–118.

Briggs, D.E.G., and E.N.K. Clarkson. 1985. Malacostracan Crustacea from the Dinantian of Foulden, Berwickshire, Scotland. Transactions of the Royal Society of Edinburgh, Earth Sciences 76: 35–40.

Briggs, D.E.G., and P.R. Wilby. 1996. The role of the calcium carbonate-calcium phosphate switch in the mineralization of soft-bodied fossils. Journal of the Geological Society 153: 665–668.

Brooks, H.K. 1962. Paleozoic Eumalacostraca of North America. Bulletins of American Paleontology 44: 163–338.

Caldwell, R.L., and M.J. Childress. 1990. Prey selection and processing in a stomatopod crustacean. *In* R.N. Hughes (editor), Behavioural mechanisms of food selection: 143–164. Berlin: Springer.

Gabbott, S.E., M.J. Norry, R.J. Aldridge, and J.N. Theron. 2001. Preservation of fossils in clay minerals; a unique example from the Upper Ordovician Soom Shale, South Africa. Proceedings of the Yorkshire Geological Society 53: 237–244.

Gunnell, F.H. 1933. Conodonts and fish remains from the Cherokee, Kansas City, and Wabaunsee groups of Missouri and Kansas. Journal of Paleontology 7: 261–297.

Haug, C., and J.T. Haug. 2021. A new fossil mantis shrimp and the convergent evolution of a lobster-like morphotype. PeerJ 9: e11124.

Haug, J.T., C. Haug, A. Maas, V. Kutschera, and D. Waloszek. 2010. Evolution of mantis shrimps (Stomatopoda, Malacostraca) in the light of new Mesozoic fossils. BMC Evolutionary Biology 10: 1–17.

Heckel, P.H. 1992. Revision of Missourian (lower Upper Pennsylvanian) stratigraphy in Kansas and adjacent states. Kansas Geologic Survey, Open-file report 92-60: 1–182.

Heckel, P.H., and J.F. Baesemann. 1975. Environmental interpretation of conodont distribution in Upper Pennsylvanian (Missourian) megacyclothems in eastern Kansas. AAPG Bulletin 59: 486–509.

Heckel, P.H., and W.L. Watney. 2002. Revision of stratigraphic nomenclature and classification of the Pleasanton, Kansas City, Lansing, and lower part of the Douglas groups (lower Upper Pennsylvanian, Missourian) in Kansas. Kansas Geological Survey Bulletin 246: 1–70.

Hershey, H.G., C.N. Brown, O. Van Eck, and R.C. Northup. 1960. Highway construction materials from the consolidated rocks of southwestern Iowa. Iowa State Highway Commission and Iowa Geological Survey, Bulletin 15: 1–151.

Hickman, C.P. 1973. Biology of the invertebrates. St Louis: CV Mosby Company.

Hof, C.H.J. 1998a. Fossil stomatopods (Crustacea: Malacostraca) and their phylogenetic impact. Journal of Natural History 32: 1567–1576.

Hof, C.H.J. 1998b. Late Cretaceous stomatopods (Crustacea, Malacostraca) from Israel and Jordan. Contributions to Zoology 67: 257–266.

Hof, C.H.J., and D.E.G. Briggs. 1997. Decay and mineralization of mantis shrimps (Stomatopoda; Crustacea); a key to their fossil record. Palaios 12: 420–438.

Jenner, R.A., C.H.J. Hof, and F.R. Schram. 1998. Palaeo- and archaeostomatopods (Hoplocarida, Crustacea) from the Bear Gulch Limestone, Mississippian (Namurian), of central Montana. Contributions to Zoology 67: 155–185.

Jauvion, C., et al. 2020. Exceptional preservation requires fast biodegradation: the case study of thylacocephalan specimens from La Voulte-sur-Rhône (Callovian, Jurassic, France). Palaeontology 63: 395–413.

Klompmaker, A.A., R.W. Portell, and M.G. Frick. 2017. Comparative experimental taphonomy of eight marine arthropods indicates distinct differences in preservation potential. Palaeontology 60: 773–794.

Latreille, P.A. 1817. Les crustacés, les arachnides et les insectes. *In* G. Cuvier (editor), Le règne animal distribué d'après son organisation: pour servir de base à l'histoire naturelle des animaux et d'introduction à l'anatomie comparée. Paris: Deterville.

Lucas, S.G., J.W. Schneider, S. Nikolaeva, and X. Wang. 2022a. The Carboniferous timescale: an introduction. Geological Society, London, Special Publications 512: 1–17.

Lucas, S.G., J.W. Schneider, S. Nikolaeva, and X. Wang. 2022b. The Carboniferous chronostratigraphic scale: history, status and prospectus. Geological Society, London, Special Publications 512: 19–48.

Martill, D.M. 1988. Preservation of fish in the Cretaceous of Brazil. Palaeontology 3: 1–18.

Meek, F.B. 1871. Descriptions of new western Palæozoic fossils, mainly from the Cincinnati Group of the Lower Silurian Series of Ohio. Proceedings of the Academy of Natural Sciences of Philadelphia 24: 308–336.

Monson, C.C. 2010. Paleontology and paleoecology of the Pennsylvanian in south-central Iowa. *In* T. Marshall and C. Fields (editors), The Pennsylvanian geology of south-central Iowa, Geological Survey of Iowa Guidebook 86: 27–35. Iowa: Geological Society of Iowa.

Moore, R.C. 1933. A reclassification of the Pennsylvanian System in the northern Mid-Continent region. *In* Guidebook, 6th regional field conference, Kansas Geological Society: 80–97. Wichita, KS: Kansas Geological Survey.

Newell, N.D. 1935. The geology of Johnson and Miami counties, Kansas. Kansas Geological Survey Bulletin 21: 1–150.

Nimchik, A., G. Pulatov, F. Yusupov, B. Haydarov, and A. Kambarov. 2024. Use of acid gases in the production of sodium sulphide. E3S Web of Conferences 494: 02003. Online resource (doi.10.1051/e3sconf/202449402003).

Orr, P.J., D.E.G. Briggs, and S.L. Kearns. 1998. Cambrian Burgess Shale animals replicated in clay minerals. Science 281: 1173–1175.

Ossian, C.R. 1973. New Pennsylvanian scyphomedusan from western Iowa. Journal of Paleontology 47: 990–995.

Patek, S.N., and R.L. Caldwell. 2005. Extreme impact and cavitation forces of a biological hammer: strike forces of the peacock mantis shrimp *Odontodactylus scyllarus*. Journal of Experimental Biology 208: 3655–3664.

Patek, S.N., M.V. Rosario, and J.R.A. Taylor. 2013. Comparative spring mechanics in mantis shrimp. Journal of Experimental Biology 216: 1317–1329.

Peach, B.N. 1881. On some new Crustaceans from the Lower Carboniferous Rocks of Eskdale and Liddesdale. Proceedings of the Royal Society of Edinburgh 30: 73–91.

Pope, J.P., and T.R. Marshall. 2010. Pennsylvanian geology of Decatur City and Thayer Quarries. *In* T. Marshall and C. Fields (editors), The Pennsylvanian geology of south-central Iowa, guidebook 86: 1–26. Iowa City, Iowa: Geological Society of Iowa.

Racheboeuf, P.R., F.R. Schram, and M. Vidal. 2009. New malacostracan Crustacea from the Carboniferous (Stephanian) Lagerstatte of Montceau-les-Mines, France. Journal of Paleontology 83: 624–629.

Schram, F.R. 1969a. Polyphyly in the Eumalacostraca? Crustaceana 16: 243–250.

Schram, F.R. 1969b. Some Middle Pennsylvanian Hoplocarida and their phylogenetic significance. Fieldiana: Geology 12: 235–289.

Schram, F.R. 1979a. The genus *Archaeocaris*, and a general review of the Palaeostomatopoda (Hoplocarida: Malacostraca). Transactions of the San Diego Society of Natural History 19: 57–66.

Schram, F.R. 1979b. The Mazon Creek biotas in the context of a Carboniferous faunal continuum. *In* M.H. Nitecki (editor), Mazon Creek fossils: 159–190. New York: Academic Press.

Schram, F.R. 1984. Upper Pennsylvanian arthropods from black shales of Iowa and Nebraska. Journal of Paleontology: 197–209.

Schram, F.R. 2007. Paleozoic proto-mantis shrimp revisited. Journal of Paleontology 81: 895–916.

Schram, F.R. 2008. An adjustment to the higher taxonomy of the fossil Stomatopoda. Crustaceana 81: 751–754.

Schram, F.R. 2010. Catalog of the fossil and recent Stomatopoda, Washington, USA. Langley, Washington: Bay Ridge Press.

Schram, F.R., and S. Koenemann. 2021. Evolution and phylogeny of pancrustacea: a story of scientific method, Oxford: Oxford University Press.

Smith, C.P.A., et al. 2023. Closing a major gap in mantis shrimp evolution-first fossils of Stomatopoda from the Triassic. Bulletin of Geosciences 98: 95–110.

Watling, L., C.H.J. Hof, and F.R. Schram. 2000. The place of the Hoplocarida in the malacostracan pantheon. Journal of Crustacean Biology 20: 1–11.

Wilby, P.R., and D.E.G. Briggs. 1997. Taxonomic trends in the resolution of detail preserved in fossil phosphatized soft tissues. Geobios 30: 493–502.

Williams, M.E. 1985. The cladodont level sharks of the Pennsylvanian black shales of central North America. Palaeontographica Abteilung A, Paläozoologie, Stratigraphie 190: 83–158.

Wortmann, U.G., R. Hesse, and W. Zacher. 1999. Major-element analysis of cyclic black shales: paleoceanographic implications for the Early Cretaceous deep western tethys. Paleoceanography 14: 525–541.

Zangerl, R., and G.R. Case. 1973. Iniopterygia: a new order of Chondrichthyan fishes from the Pennsylvanian of North America. Fieldiana 6: 1–66.

All issues of *Novitates* and *Bulletin* are available on the web (https://digitallibrary.amnh.org/handle/2246/5). Order printed copies on the web from:
https://shop.amnh.org/books/scientific-publications.html

or via standard mail from:
American Museum of Natural History—Scientific Publications
Central Park West at 79th Street
New York, NY 10024

♾ This paper meets the requirements of ANSI/NISO Z39.48-1992 (permanence of paper).